# Testing of surface properties pre-rad and post-rad of n-in-p silicon sensors for very high radiation environment

S. Lindgren [m], A.A. Affolder [h], P.P. Allport [h], R. Bates [e], C. Betancourt [m,*], J. Bohm [l], H. Brown [h], C. Buttar [e], J.R. Carter [b], G. Casse [h], H. Chen [a], A. Chilingarov [g], V. Cindro [i], A. Clark [d], N. Dawson [m], B. DeWilde [o], F. Doherty [e], Z. Dolezal [k], L. Eklund [e], V. Fadeyev [m], D. Ferrèrre [d], H. Fox [g], R. French [n], C. García [q], M. Gerling [m], S. Gonzalez Sevilla [d], I. Gorelov [j], A. Greenall [h], A.A. Grillo [m], N. Hamasaki [p], K. Hara [p], H. Hatano [p], M. Hoeferkamp [j], L.B.A. Hommels [b], Y. Ikegami [f], K. Jakobs [c], J. Kierstead [a], P. Kodys [k], M. Köhler [c], T. Kohriki [f], G. Kramberger [i], C. Lacasta [q], Z. Li [a], D. Lynn [a], P. Maddock [m], I. Mandić [i], F. Martinez-McKinney [m], S.Martíi Garcia [q], R. Maunu [o], R. McCarthy [o], J. Metcalfe [j], M. Mikestikova [l], M. Mikuž [i], M. Miñano [q], S. Mitsui [p], V. O'Shea [e], U. Parzefall [c], H.F.-W. Sadrozinski [m], D. Schamberger [o], A. Seiden [m], S. Terada [f], S. Paganis [n], D. Robinson [b], D. Puldon [o], S. Sattari [m], S. Seidel [j], K. Toms [j], D. Tsionou [n], Y. Unno [f], J. Von Wilpert [m], M. Wormald [h], J. Wright [m], M. Yamada [p]

[a] Brookhaven National Laboratory, Physics Department and Instrumentation Division, Upton, NY 11973-5000, USA
[b] Cavendish Laboratory, University of Cambridge, JJ Thomson Avenue, Cambridge CB3 0HE, UK
[c] Physikalisches Institut, Universität Freiburg, Hermann-Herder-Street 3, D-79104 Freiburg, Germany
[d] Section de physique, Universite de Geneve, 24, rue Ernest Ansermet CH-1211 Geneve, Switzerland
[e] Department of Physics and Astronomy, University of Glasgow, Glasgow G12 8QQ, UK
[f] KEK, High Energy Accelerator Organization, INPS, 1-1 Oho, Tsukuba, Ibaraki 305-0801, Japan
[g] Physics Department, Lancaster University, Lancaster LA1 4YB, UK
[h] Oliver Lodge Laboratory, Department of Physics, University of Liverpool, Oxford Street, Liverpool L69 7ZE, UK
[i] Jožef Stefan Institute, Department of Physics, University of Ljubljana, Ljubljana, Slovenia
[j] Department of Physics and Astronomy, University of New Mexico, MSC07 4220 800 Yale Blvd. NE Albuquerque, NM 87131, USA
[k] Faculty of Mathematics and Physics, Charles University in Prague, V Holesovickach 2 Prague 8, Czech Republic
[l] Institute of Physics, Academy of Sciences of the Czech Republic, Na Slovance 2, 18221 Prague 8, Czech Republic
[m] SCIPP, UC Santa Cruz, CA 95064, USA
[n] Department of Physics and Astronomy, The University of Sheffield, Hicks Building, Hounsfield Road, S3 7RH Sheffield, UK
[o] Department of Physics and Astronomy, Stony Brook University, Tony Brook, NY 11794-3800, USA
[p] School of Pure and Applied Sciences, University of Tsukuba, 1-1-1 Tennodai, Tsukuba, Ibaraki 305-8571, Japan
[q] IFIC (Centro Mixto CSIC-UVEG), Edificio Investigacion Paterna, Apartado 22085 46071 Valencia, Spain

## ARTICLE INFO

## ABSTRACT

We are developing $n^+$-in-p, p-bulk and n-readout, microstrip sensors as a non-inverting radiation hard silicon detector for the ATLAS Tracker Upgrade at the super LHC experiment. The surface radiation damages of the sensors fabricated by Hamamatsu Photonics are characterized on the interstrip capacitance, interstrip resistance and punch-through protection evolution. The detector should provide acceptable strip isolation, exceeding the input impedance of the signal readout chip $\sim 1\,k\Omega$, after the integrated luminosity of $6\,ab^{-1}$, which is twice the luminosity goal.

Published by Elsevier B.V.

## 1. Introduction

The silicon microstrip detector continues to play an essential role in high-energy experiments for its ability of precision tracking. The detector at the planned Super LHC (large hadron collider) is required to remain operational up to the integrated luminosity of $3000\,fb^{-1}$ with the instantaneous luminosity of $1 \times 10^{35}\,cm^{-2}\,s^{-1}$. In order to cope with ten-fold increase in instantaneous luminosity beyond the design value of the LHC, currently under commissioning, the ATLAS collaboration is investigating an inner tracking system based fully on semiconductor devices. The segmentation is varied in radius $R$, the innermost being the pixel, followed by short (2.4 cm) and long (9.7 cm) microstrip detectors. The radiation activity [1] with a

* Corresponding author. Tel.: +1 831 459 3567; fax: +1 831 459 5777.
E-mail address: cbetanco@ucsc.edu (C. Betancourt).

safety factor of two multiplied is $(7-11) \times 10^{14}$ 1 MeV $n_{eq.}/cm^2$ for the short strip ($R=38$ cm) and $3-6 \times 10^{14}$ 1 MeV $n_{eq}/cm^2$ for the long strip ($R=85$ cm) regions, where the two numbers in the parentheses are the fluence values at the central and forward regions. The charged particle contribution to the fluence is similar to the neutral at $R\sim28$ cm in the central region but decreases with $R$ and in the forward region to typically 20% of the total. It is therefore important to investigate the damages due to both charged particles and neutrons. Both neutrons and protons displace silicon atoms via non-ionizing energy losses, which results in a bulk damage. Protons in addition ionize the atoms in their path that leads to permanent damage at the sensor surface.

The ATLAS R&D group "Development of non-inverting silicon strip detectors for the ATLAS ID upgrade" is formed to develop radiation hard tracking detectors based on the p-bulk microstrip [2] technology. Since the radiation induced impurity in silicon acts as an acceptor, the $n^+$-on-p device is non-inverting. This allows us to operate the sensors at partial depletion when obliged. The experience of adopting p-bulk silicon for particle tracker is limited. This is in part because additional strip isolation structure is required for individual strip signal readout to prevent mobile electrons to be accumulated between strips. The R&D group is evaluating the sensors fabricated by Hamamatsu Photonics using commercially available p-type wafers. We report the surface damage including the decrease in strip isolation and punch-through voltage evolution. The bulk damage is reported in Ref. [3].

One of the most pressing issue for n-in-p strip sensors are the interstrip characteristics before and after ionizing radiation, since the electron accumulation layer on the surface needs to be compensated for large fluences and dose levels.

Previous studies with p-type sensors, e.g. within the context of RD50, were done using p-spray to isolate the n-strips [4]. This study uses "mini-SSDs" ($\sim 1$ cm long) produced by Hamamatsu Photonic (HPK) within the ATLAS upgrade program. The isolation is done with p-stops of varying geometry, p-spray and both combined with p-doses (concentration) varying from 0 up to $2 \times 10^{13}$ p/cm$^2$.

## 2. Samples and irradiation

The sample sensors were fabricated using 15 cm wafers with $\langle 1\,0\,0 \rangle$ crystal orientation and 320 μm thickness. The wafers we report in this paper are FZ grown (FZp wafers in Ref. [5]) having fewer defects than normal FZ wafers. The R&D group continues to evaluate other commercially available p-type wafers [5]. The strip pitch is 74.5 μm. Details of the design including strip isolation structures are described in Ref. [2]. The performance of main sensors, 97.5 mm$^2$, is reported elsewhere [6]. The characteristics of irradiated sensors are studied using miniature samples of 10 mm square, where there are 104 strips of 8 mm length.

The proton irradiation was performed at Cyclotron Radio Isotope Center (CYRIC) of Tohoku University. Details of irradiation facility and methods are described in Refs. [5,7]. 70-MeV protons were uniformly irradiated by scanning periodically the sample sensors. The irradiation took typically a few 10 min to a few hours depending on the fluence. The sensors were kept cooled at $-10°$ C during irradiation and the irradiated samples were immediately stored in refrigerator to suppress any post-irradiation annealing to take place. The samples measured in Japan were glued on printed circuit board and biased at $-100$ V during the irradiation. The samples measured elsewhere were irradiated as bare chips with no bias applied. The fluence we refer to is in 1 MeV neutron equivalent value taking into account the NIEL factor of 1.4. The fluence uncertainty is determined by the $^{27}$Al(pn) reaction cross-section, which does not exceed 10%.

## 3. Strip isolation structures

It is thought that n-on-p detectors are more sensitive to surface effects than p-on-n detectors. One concern is the risk that the fixed oxide charges in the Si–SiO$_2$ interface would lead to a conductive layer of electrons at the surface [8]. Within the project ATLAS07 for the ATLAS upgrade different structures for mini-SSDs have been produced. The different structures use the concept of preventing those damages by surface treatments, positive doped implants (p-impurities) in form of p-stop or p-spray, or combinations of both.

The p-stops are implanted to the detectors with a mask while p-spray is sprayed on over the whole sensor. Several doses and combinations of p-stop and p-spray have been applied to different sensors. Different structures to apply the p-stops have also been used, which is indicated by different zone number and seen in Fig. 1.

Detectors with zone 1 have no structure, i.e. they have only p-spray since the p-stop mask was left out. Detectors with zone 2 have individual p-stops, i.e. each strip is surrounded by p-implants in opposite to the other structures which only have a line of common p-implants between the strips. Zone 3 shares the p-stops between the strips and zone 4 has additional punch-through protection structure, which will be discussed later in the paper. Detectors with zone 5 have narrow metal, meaning the aluminum layer over the strips do not reach outside the strip itself and finally zone 6 is similar to zone 3 but with a wider strip pitch.

## 4. Interstrip resistance and capacitance measurements

The interstrip resistance and capacitance are important parameters used to characterize the effects of surface radiation damage of silicon strip detectors. The interstrip resistance is important for strip isolation, so that a sufficiently high interstrip resistance can prevent signal sharing between neighbors which could lead to degradation of the position resolution. The interstrip capacitance is the main contributor of noise in between strips. A properly functioning detector should thus try to minimize the interstrip capacitance in order to have a higher signal-to-noise ratio, while maximizing the interstrip resistance to minimize crosstalk between strips.

Interstrip resistance measurements were performed in a probe station. As seen in Fig. 2, the DC pad of a test strip was connected to an Agilent 4156C Precision Semiconductor Parameter Analyzer and grounded while a voltage $V_2$ was applied to the DC pads of two of its closest neighbors, which were also connected to the analyzer. The detectors were biased using a Keithley 2410HV Source Meter and each measurement was performed at several bias voltages ranging from 5 to 300 V. The voltage $V_2$ applied to the neighbor strips was varied through the parameter analyzer from $-1$ to 1 V in 100 mW steps. Each measurement was performed at $22°$ C with nitrogen gas flowing over the detector for moisture control.

The idea is that the voltage $V_2$ on the neighbors will induce a current $I_1$ through the test strip. The interstrip resistance can then be determined by

$$R_{int} = 2dV_2/dI_1 \tag{1}$$

where the factor of 2 comes from the fact that two neighboring strips are used. The resulting IV curve is shown in Fig. 3.

To measure the interstrip capacitance a slightly different set-up was used. Instead of using the DC pads, the test strip and its neighbors were connected to an Agilent E4980A Precision LCR meter via the AC pads. In addition, the next two neighbors (two strips away from the test) were grounded to act as a shield from
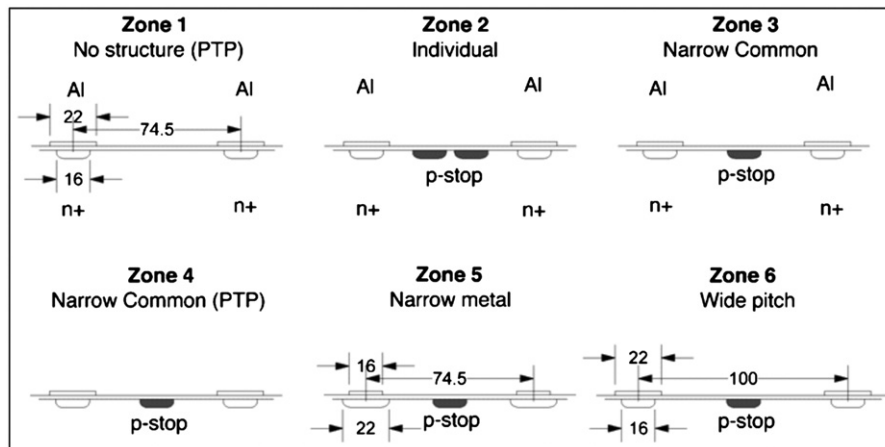
**Fig. 1.** Different p-stop structures as indicated by the different zone numbers.
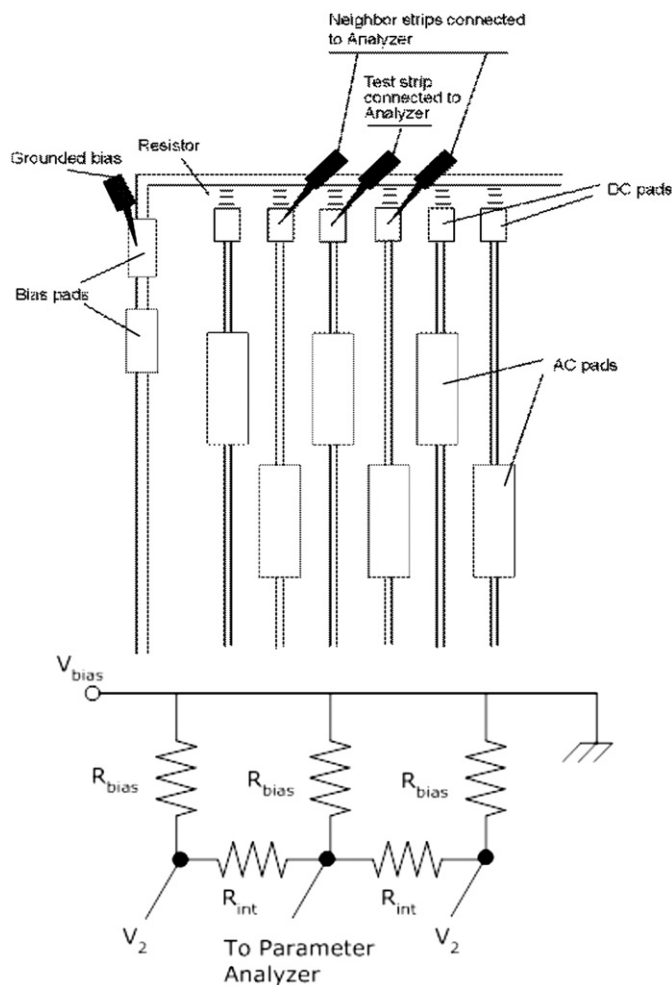


**Fig. 2.** Measurement set-up for interstrip resistance. Visual illustration of the measurement (top), showing the connections to the strips via the DC pads and to the bias ring. An equivalent circuit diagram (bottom) is also displayed.
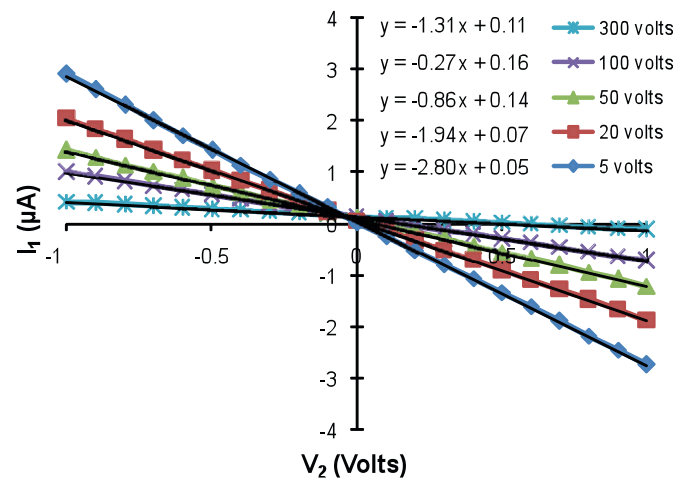


**Fig. 3.** The current through the test strip vs. the voltage applied to the neighbors shown at different bias votlages. The interstrip resistance is given by the inverse of the slope.

the outer laying strips. The frequency of the AC signal from the LCR meter was varied, and each measurement was taken at 10 kHz, 100 kHz, 1 MHz, and 2 MHz. The bias voltage ranged from 0 to −800 V with a step size of 50 V. The measurements were again performed at 22° C with nitrogen gas flowing over the detector.

## 5. Punch-through protection

Ac-coupled sensors are susceptible to very large voltages between the metal readout traces (held to ground through the front-end electronics) and the strip implants in the case of large charge accumulation in the bulk, for instance in the case of beam losses [9]. When sufficient charge is deposited in the detector, the electric field can collapse causing the implants and backplane of the sensor to float to unknown voltages. These large voltages on the implants can reach the order of half the bias voltage, and thus can exceed the specification for the hold-off voltage of the coupling capacitor, which are typically tested to 100 V. In order to prevent these large voltages, the punch-through (reach-through) effect is used [10], where implants in close proximity will effectively be shorted together if the voltage between them exceeds a geometry dependent voltage. This provides an effective over-voltage protection for single strips, which get shorted to the bias line in the case of voltages in excess of the punch-though protection ("PTP") voltage.

Protection against large voltages between strip implants and the metal traces can be achieved with the punch-through effects between strips and bias ring. This is trivially done for p-spray, but requires sophisticated structures in the case of p-stops. In this paper, the effects of several PTP structures on the PTP voltage

have been studied. In particular, zone 4 detectors were designed with complicated PTP structures, as seen in Fig. 4.

Unirradiated detectors were measured at Lancaster University in a probe station kept at 21°C. Measurements on irradiated detectors were carried out at the University of Tsukuba where detectors were placed two at a time on printed circuit boards which were then placed in a thermostat chamber set at −20°C with nitrogen gas flowing in for moisture control.

For PTP measurements, the effective resistance is measured between the DC pad of a strip and the bias ring. The detectors were reverse biased to 300 V with voltage being applied to the backplane and the bias ring grounded. A test voltage $V_{test}$ is then applied to the DC pad, and the subsequent induced $I_{test}$ current was measured between the pad and the bias ring. The neighboring strips were left floating. The effective resistance is then given by

$$R_{eff} = dV_{test}/dI_{test}. \tag{2}$$

The effective resistance can be thought of as the bias resistor in parallel to another resistance, which we call the punch-through resistance. The effective resistance can then be written as

$$R_{eff} = (1/R_{bias} + 1/R_{PT})^{-1} \tag{3}$$

where $R_{bias}$ is value of the bias resistor and $R_{PT}$ is the punch-through resistance.

The punch-through voltage $V_{PT}$ is then taken to be the voltage where

$$R_{PT} = R_{bias} \tag{4}$$

or alternatively the point where the effective resistance is equal to half the value of the bias resistor. The effective resistance as a function of the test voltage for an unirradiated detector is shown in Fig. 5a while irradiated detectors are shown in Fig. 5b.

## 6. Results

To first order, the interstrip resistance does not seem to depend on the specific zone, but instead depends only on the total amount of p-dose applied to the surface (through p-stop or p-spray), as seen in Fig. 6. There is an obvious correlation between the total amount of p-dose applied and the value of interstrip resistance after irradiation, with a higher total p-dose resulting in better post-rad strip isolation (higher interstrip resistance), which is illustrated in Fig. 7.
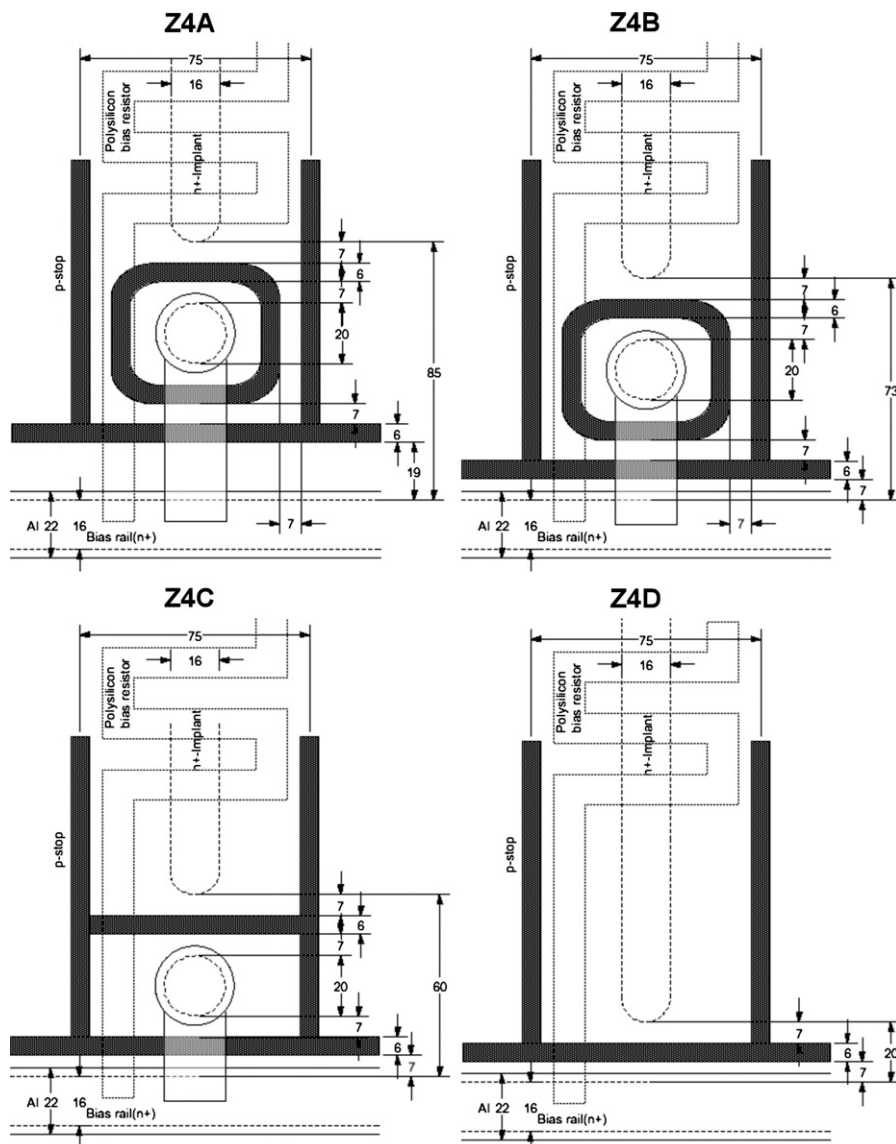


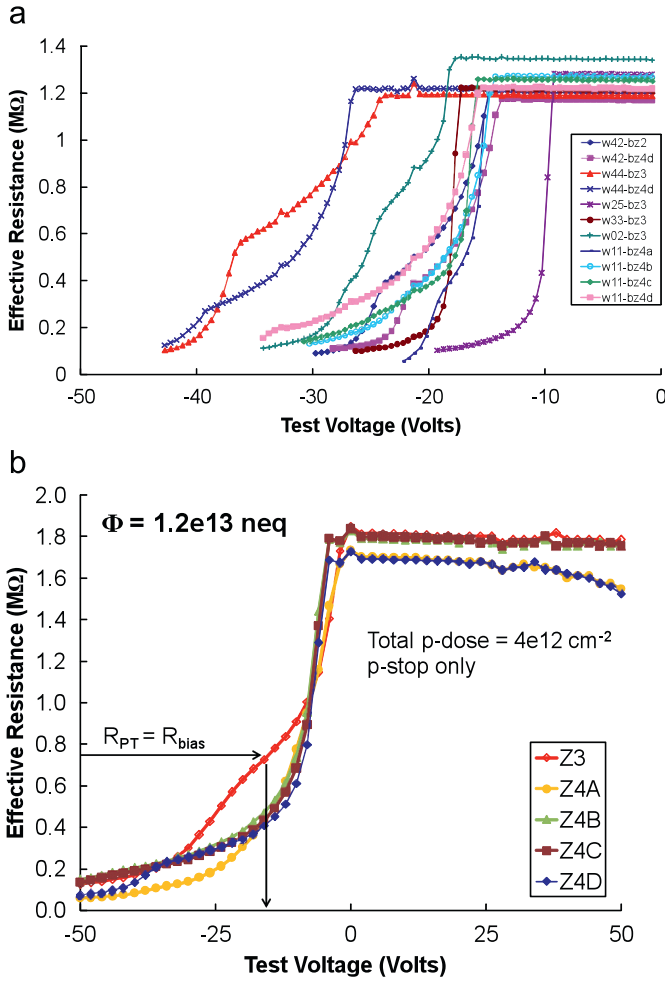Fig. 4. The different PTP structures designs that have been tested for the paper.

a



b

**Fig. 5.** The effective resistance vs. the test voltage applied for (a) unirradiated detectors and for (b) detectors irradiated with protons to $1.2 \times 10^{13}$ $n_{eq}$. The horizontal arrow indicates where the punch-through resistance is equal to the value of bias resistor, and the vertical arrow indicates the corresponding punch-through voltage.
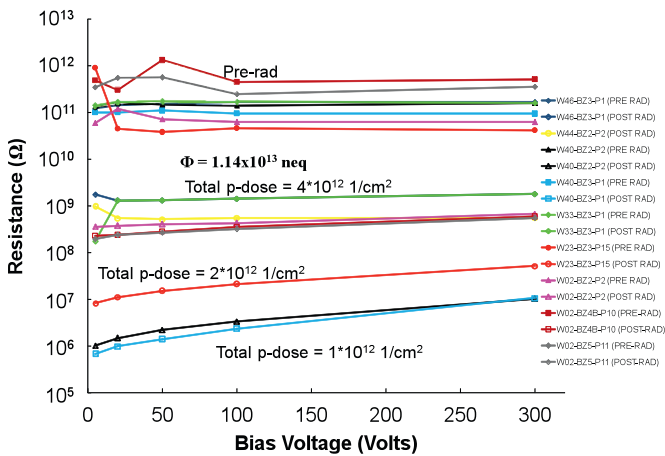


**Fig. 7.** Interstrip resistance vs. the total p-dose applied for detectors irradiated with protons to $1 \times 10^{13}$ $n_{eq}$. Higher p-doses lead to higher interstrip resistance after irradiation.
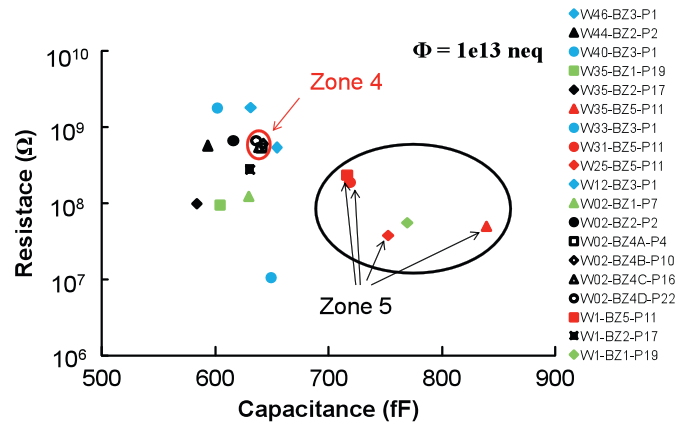


**Fig. 8.** Scatter plot of the interstrip resistance vs. interstrip capacitance for detectors irradiated to $1 \times 10^{13}$. Zone 5 (black circle) tends to perform the worst compared with the other zones.



**Fig. 6.** Interstrip resistance for irradiated series 3 detectors. There is a clear dependence on the total p-dose applied after irradiation.

The interstrip capacitance shows little change after irradiation, and seems to be dependent on the specific zone, but not really on the amount of total p-dose applied. Still, the dependence is weak,

and no predictions could be made about whether adding a p-stop mask would increase or decrease, or by which amount, the interstrip capacitance. Zone 5 is the only exception to this, consistently showing an increase in capacitance after irradiation.

It is helpful to plot the interstrip resistance vs. the interstrip capacitance. This helps determine which detectors have the most favorable behavior (the highest resistance and the lowest capacitance). Detectors performing the best should lie in the upper-left corner of the graph, while the least preferable behavior is seen in the lower-right of the graph. Fig. 8 shows the interstrip resistance vs. capacitance for several detectors of different zones and total p-dose. One can see that zone 5 tends to have the worst interstrip properties after irradiation.

The leakage current as a function of the bias voltage was measured in order to determine if good strip isolation came with the disadvantage of a lower breakdown voltage. The IV curves for various irradiated detectors taken at room temperature are shown in Fig. 9. It can be seen that all most detectors have a breakdown voltage in excess of 1000 V, while three detectors (all zone 3) exhibit breakdown at about 900 V. The high breakdown voltage should not significantly affect our measurements, as the interstrip resistance is taken at 300 V, and the capacitance at 800 V, which are both safely below the breakdown voltage. It is also important to note that all detectors exhibit breakdown at a much higher
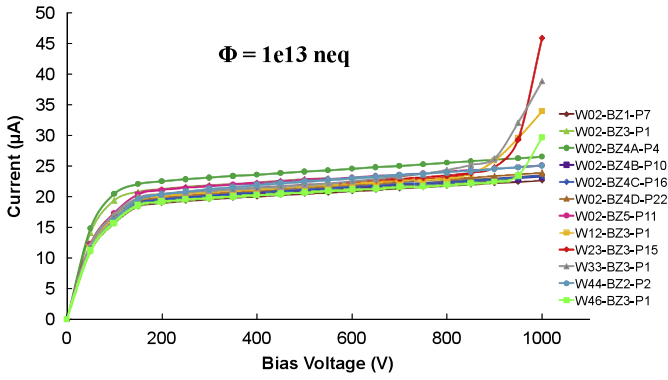
**Fig. 9.** Leakage current vs. bias voltage for various detector types irradiated to $1 \times 10^{13}$ $n_{eq.}$ taken at 22 °C. Zone 3 breaks down the earliest at $\sim 900$ V, which is still greater than the 600 V breakdown specified by the manufacturer.
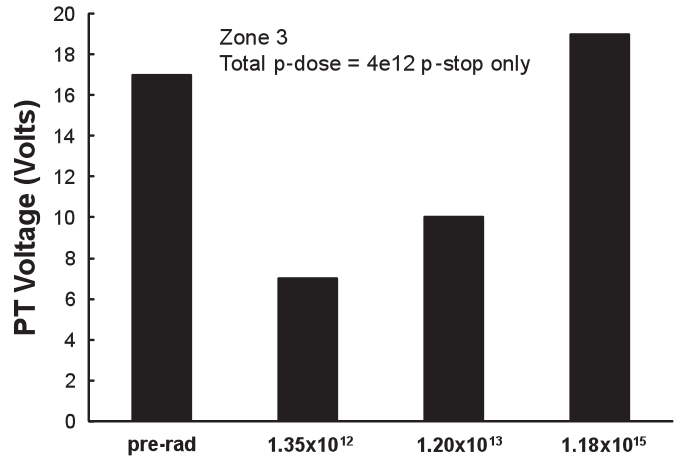


**Fig. 11.** Punch-through voltage for zone 3 measured at various fluences. Total p-dose $= 4 \times 10^{12}$ cm$^{-2}$, fluence values are in $n_{eq}$.

It is interesting to note that the punch-through voltage for zone 3 detectors and zone 4 detectors is similar before and after irradiation. This implies that the complicated punch-through protection structures are not needed, as zone 3, which has a distance of 70 μm from the n+ implant to the bias rail, seems to provide adequate protection. Further, as seen in Fig. 11, zone 3 detectors exhibit adequate protection even at high fluences, having a punch-through voltage in the range of 7–20 V. This further suggests that complicated punch-through protection structures are not necessary.
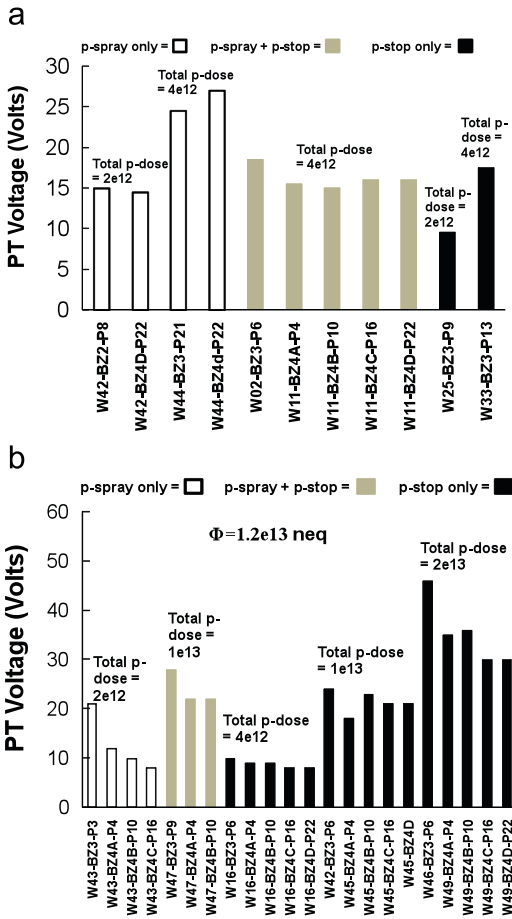




**Fig. 10.** Punch-through voltage for (a) unirradiated detectors and (b) detectors irradiated to $1.2 \times 10^{13}$ $n_{eq}$. Both pre and post-rad detectors show a dependence on the total p-dose applied.

voltage than the breakdown voltage of 600 V that was specified by the manufacturer.

The punch-through voltage for unirradiated detectors is between 10 and 30 V, as seen in Fig. 10a. There seems to be a clear wafer correlation on the value of the punch-through voltage, i.e. the voltage depends on the total p-dose and type (p-spray, p-stop). After irradiation, a dependence of the punch-through voltage on the total p-dose and type is still evident, which is seen in Fig. 10b.

## 7. Summary and discussion

We are designing radiation hard silicon microstrip detector for the ATLAS Inner Detector Upgrade at the super LHC. P-bulk sensor is a good candidate for such a very high radiation environment reaching $1 \times 10^{15}$ 1 MeV $n_{eq}$/cm$^2$.

The interstrip resistance decreases and interstrip capacitance increases after irradiation. To first order, the interstrip resistance does not depend on the specific zone of the detector, but instead depends on the total dose of the p-impurities applied. The higher the total doses of impurities, the better the strip isolation that can be achieved after irradiation. The interstrip capacitance shows little change after irradiation and is dependent on the specific zone. Specifically, zone 5, which has narrow metal, tends to have the highest interstrip capacitance after irradiation, without providing any benefits such as a higher breakdown voltage. The higher interstrip capacitance for zone 5 is not surprising given the shorter distance between readout strips compared with other zones.

Even if the interstrip resistance is low, one would only expect to see a loss in signal and increase in noise if the values were on the same order of magnitude as input impedance of the signal readout chip, which is typically about 1 kΩ. The signal gets coupled to the metal strip and to the amplifier instead of being shorted to the neighbor via the DC conductance. Therefore, as long as the interstrip resistance is large compared to the input impedance of the chip, the signal will end up in the amplifier. Further, there has not yet been any observed signal degradation or noise increase due to a decrease in the interstrip resistance.

The breakdown voltage for zone 3 detectors tends to start at slightly lower voltages than other detectors, but the voltage is above 900 V and is much greater than the 600 V breakdown voltage specified by the manufacture.

Measurements of the punch-through voltage reveal that there is a clear wafer correlation. In particular, when looking at a specific configuration (p-spray only, p-stop only, p-spray+stop) wafers with the highest p-dose have the highest punch-through voltage, which holds true even after irradiation.

After irradiation, zone 3 detectors have similar punch-through voltages as zone 4 detectors, which have a much more complicated punch-through protection structure. The acceptable punch-through voltage of zone 3 detectors with p-stops of $4 \times 10^{12}$ cm$^{-2}$ extends to proton fluences beyond $10^{15}$ p/cm$^2$. Thus, punch-through protection is achievable with zone 3 which has no dedicated structure.

It is important to mention that Eq. (2) is not the only way to define $R_{eff}$. An alternate definition would be to take the integral form of Eq. (2). This would have the advantage of incorporating the total current that can be drained from the strip to the bias rail and providing the effective resistance for charges to escape through. But the integral definition is less sensitive to the onset of punch-though, and thus less suitable for finding the onset of the punch-though voltage. This leads to a higher punch-through voltage, culminating in differences between 5 and 30 V from the definition used in this paper.

## Acknowledgements

## References

[1] I. Dawson, Radiation predictions at the SLHC and irradiation facilities, ATLAS Tracker Upgrade Workshop, Liverpool, 6–8 December 2006. Available from: ⟨http://dawson.web.cern.ch/dawson/fluka/index.html⟩.
[2] Y. Unno, et al., Development of n-on-p silicon sensors for very high radiation environment, Nucl. Instr. and Meth. A, this issue.
[3] K. Hara, et al., Testing of bulk radiation of n-in-p silicon sensor for very high radiation environment, Nucl. Instr. and Meth. A, this issue.
[4] C. Casse, Nucl. Instr. and Meth. A 535 (2004).
[5] K. Hara, et al., IEEE Trans. Nucl. Sci. NS-56(2) (2009) 468.
[6] M. Mikestikova, et al., Testing of large area n-in-p silicon sensors intended for very high radiation environment, Nucl. Instr. and Meth. A, this issue.
[7] Y. Unno, et al., Nucl. Instr. and Meth. A 579 (2007) 614.
[8] H.F.W. Sadrozinski, et al., Nucl. Instr. and Meth. A 579 (2007) 769–774.
[9] T. Dubbs, M. Harms, H.F.W. Sadrozinski, A. Seiden, M. Wilson, IEEE Trans. Nucl. Sci. NS-47(6) (2000) 1902.
[10] J. Ellison, et al., IEEE Trans. Nucl. Sci. NS-36(1) (1989) 267.